Inorganic Chemistry
Article

Inorg. Chem. **2009**, *48*, 9779–9785 **9779**
DOI: 10.1021/ic901368t

Synthesis, Structures, Spectroscopic and Electrochemical Properties of Dinitrosyl Iron Complexes with Bipyridine, Terpyridine, and 1,10-Phenathroline

Rongming Wang,[†] Ximeng Wang,[†] Eric B. Sundberg,[†] Phuongmei Nguyen,[†] Gian Paola G. Grant,[†] Chaitali Sheth,[†] Qiang Zhao,[‡] Steve Herron,[‡] Katherine A. Kantardjieff,[‡] and Lijuan Li*[,†]

[†]*Department of Chemistry and Biochemistry, California State University, Long Beach, California 90840, and* [‡]*Department of Chemistry and Biochemistry and the W.M. Keck Foundation Center for Molecular Structure, California State University, Fullerton, California 92831*

Received July 13, 2009

Three new dinitrosyl iron complexes $LFe(NO)_2$ (L = 2,2′-bipyridine (bipy) (**1**), 2,2′,2″-terpyridine (terpy) (**2**) and 1,10-phenathroline (phen) (**3**)) were synthesized by the reaction of $Fe(NO)_2(CO)_2$ with corresponding ligands in tetrahydrofuran. Complexes **1**−**3** were studied using IR, UV−vis, MS, NMR, and electrochemical techniques. Complexes **1** and **2** were also characterized using single crystal X-ray diffraction analysis. IR spectra of complexes **1**−**3** display two strong characteristic NO stretching frequencies (ν_{NO}) in the region reflecting donor properties of the ligands. Cyclic voltammetry studies show two quasi-reversible one-electron reductions for all complexes. Electrochemical investigations using different concentrations show that an irreversible one-electron reduction at −1.85 V for complex **2** and −1.80 V for complex **3** are from solvated species. Single-crystal X-ray structural analysis reveals that complex **1** crystallizes in the triclinic $P\bar{1}$ space group and the asymmetric unit consists of one $Fe(NO)_2$(bipy) molecule with the two NO groups located on two sides of Fe(bipy) plane. Complex **2** crystallizes in monoclinic $P21/n$ space group, and the asymmetric unit contains one $Fe(NO)_2$(terpy) molecule, in which the NO groups are located on two sides of the plane consisted of Fe and two coordinated pyridyl rings, but almost parallel to the uncoordinated pyridyl ring. The crystal packings of both complexes **1** and **2** show intermolecular H-bonding and strong $\pi-\pi$ stacking interactions.

Introduction

Nitric oxide's specific roles in many physiological functions remain unclear. A number of attempts to fully elucidate these functions have revealed the involvement of iron dinitrosyls. Dinitrosyl iron complexes (DNICs) which are protein-bound have a typical $g_{av} = 2.03$ electron paramagnetic resonance (EPR) signal. This has been observed in the process of the degradations of the *C. botulinum* iron−sulfur proteins and the *C. Vinosum* high potential iron protein (HIPIP-type iron−sulfur protein).[1] DNIC $Cys_2Fe(NO)_2$ is formed when the immune system utilizes NO to combat intracellular pathogens in cells.[2] Endothelium-derived relaxing factor (EDRF), responsible for relaxing blood vessels, stabilizes NO in cells, facilitates the transfer of NO into tissues, and releases the radical in its active free state, was found to be a DNIC.[3] Muller et al. and others have observed non-heme DNICs acting as NO storage molecules.[4] Lee et al. identified three types of EPR-active non-heme iron nitrosyl complexes in mammalian ferritins, which have been attributed to iron nitrosyl complexes with imidazole groups of histidine, thiol groups of cysteine, or carboxylate groups of aspartate and glutamate.[5]

These recent developments involving the physiological implications of nitric oxide have spurred intense interest in transition metal nitrosyl complexes, especially those that mimic the structures of biologically active metal-nitrosyl complexes.[6] A large number of DNICs containing amino

*To whom correspondence should be addressed. E-mail: lli@csulb.edu.

(1) (a) Reddy, D.; Lancaster, J. R.; Cornforth, D. P. *Science* **1983**, *221*, 769–770. (b) Challis, B. C.; Milligan, J. R.; Mitchell, R. C. *J. Chem. Soc., Chem. Commun*. **1984**, 1050–1051. (c) Foster, M. W.; Cowan, J. A. *J. Am. Chem. Soc*. **1999**, *121*, 4093–4100.

(2) (a) Vanin, A. F.; Varich, V. Y. *Stud. Biophys*. **1981**, *86*, 177–179. (b) Lancaster, J. R., Jr.; Hibbs, J. B., Jr. *Proc. Natl. Acad. Sci. U.S.A*. **1990**, *87*, 1223–1227. (c) Feldman, P. L.; Griffith, O. W.; Stuehr, D. J. *Chem. Eng. News* **1993**, *71*, 26–38.

(3) Vanin, A. F. *FEBS Lett*. **1991**, *289*, 1–3.

(4) (a) Butler, A. R.; Flitney, F. W.; Williams, D. L. H. *Trends Pharmacol. Sci*. **1995**, *16*, 18–22. (b) Noguchi, T.; Honda, J.; Nagamune, T.; Sasabe, H.; Inoue, Y.; Endo, I. *FEBS Lett*. **1995**, *358*, 9–12. (c) Muller, B.; Kleschyov, A. L.; Stoclet, J. C. *Br. J. Pharmacol*. **1996**, *119*, 1281–1285.

(5) Lee, M.; Arosio, P.; Cozzi, A.; Chasteen, N. D. *Biochem*. **1994**, *33*, 3679–3687.

(6) (a) Odaka, M.; Fujii, K.; Hoshino, M.; Noguchi, T.; Tsujimura, M.; Nagashima, S.; Yohda, N.; Nagamune, T.; Inoue, I.; Endo, I. *J. Am. Chem. Soc*. **1997**, *119*, 3785–3791. (b) Foster, M. W.; Cowan, J. A. *J. Am. Chem. Soc*. **1999**, *121*, 4093–4100. (c) Chiang, C.-Y.; Miller, M. L.; Reibenspies, J. H.; Darensbourg, M. Y. *J. Am. Chem. Soc*. **2004**, *126*, 10867–10874. (d) Harrop, T. C.; Song, D.; Lippard, S. J. *J. Am. Chem. Soc*. **2006**, *128*, 3528–3529. (e) Wecksler, S. R.; Mikhailovsky, A.; Korystov, D.; Buller, F.; Kannan, R.; Tan, L.; Ford, P. C. *Inorg. Chem*. **2007**, *46*, 395–402.

© 2009 American Chemical Society
Published on Web 09/21/2009

acids, peptides, and thiol ligands have been synthesized and proven to be useful in serving as structural models for active sites in iron sulfur proteins.[6c,7,8] However, very few structures of isolated DNICs containing N-donor ligands have been reported.[9] The trend has been to detect the presence of these compounds by IR and EPR rather than to isolate them, because isolation and structural determination of these compounds are extremely tedious and difficult. In the search of literature precedent in the area of isolated DNICs with N, N′-chelating ligands, we found very limited examples that exist despite the fact that coordination of N,N′-chelating ligands to transition metals is very common.[11] It was reported that reaction of $[Fe(NO)_2Cl]_2$ with a bidentate nitrogen ligand, 1,4,-diaza-1,3-butadiene (R−N=CR′−CR′=N−R) yielded a DNIC with N,N′-chelation.[7d] Another example involved 2,2′-bipyridine, in which a salt $[Fe(bipy)_3][Fe(NO)_2Cl_2]_2$ was isolated by using large excess of bipy versus $[Fe(NO)_2Cl]_2$ (10:0.75).[12] A third, [(spartiene)$Fe(NO)_2$] was prepared by reacting spartiene with $Fe(CO)_2(NO)_2$.[10] In our continuing interest in non-heme iron nitrosyl model complexes,[9a,b,13] here we report the synthesis, structures, spectroscopic and electrochemical properties of three new DNICs with bidentate [N,N] chelating ligands; 2,2′-bipyridine (bipy) (**1**), 2,2′,2″-terpyridine (terpy) (**2**), and 1,10- phenathroline (phen) (**3**). The isolation and investigation of this new class of compounds help us to gain an insight on the structures of non-heme iron nitrosyls and establish the important relationship between structures and functions of these molecules in biological systems.

Experimental Section

Materials and Methods. $Fe(NO)_2(CO)_2$ was synthesized according to the reported procedure.[14] Other chemicals were purchased from Aldrich Chemical Co. and were used without further purification. All solvents were purified and/or dried by standard techniques and degassed under vacuum prior to use. IR spectra were recorded on a Nicolet AVATAR 380 FT-IR infrared spectrophotometer. UV−visible spectra were measured on a Varian Cary 300 Bio UV−visible spectrophotometer. Mass spectra were obtained with a Finnigan MAT 95 MS spectrometer. The ^{1}H- and ^{13}C NMR spectra were obtained on a Bruker 400 MHz NMR spectrometer, using tetramethylsilane as an internal standard.

Table 1. Crystallographic Collection and Refinement Parameters for Complexes **1** and **2**

	1	**2**
formula	$C_{10}H_8FeN_4O_2$	$C_{15}H_{11}FeN_5O_2$
M_r	272.05	349.14
crystal color	red	red
crystal system	triclinic	monoclinic
space group	$P\bar{1}$	$P21/n$
a [Å]	7.556(3)	7.2063(8)
b [Å]	8.991(3)	12.7208(13)
c [Å]	9.222(3)	16.4642(18)
α [deg]	75.979(5)	90
β [deg]	70.327(5)	98.926(4)
γ [deg]	70.099(5)	90
V [Å^3]	548.9(3)	1491.0(3)
Z	2	4
F(000)	276	712
ρcalcd [g cm^{-3}]	1.646	1.555
[mm^{-1}]	1.368	1.028
range [deg]	2.37 to 28.20	2.03 to 23.30
reflec. collected	4259	2144
indep. reflec.	3705 (R_{int} = 0.0358)	1801 (R_{int} = 0.0359)
parameters	252	217
$R1$ [$I > 2\sigma(I)$]	0.0460	0.0460
$wR2$ [$I > 2\sigma(I)$]	0.1498	0.0722
goodness of fit	1.218	1.162

Synthesis of Complex 1. A mixture of $Fe(NO)_2(CO)_2$ (0.1 mL, 0.9 mmol) and 2,2′-bipyride (140 mg, 0.9 mmol) in tetrahydrofuran (THF, 5 mL) was stirred 48 h at ambient temperature under nitrogen atmosphere. At the beginning, a great amount of bubbles was produced upon the addition of $Fe(NO)_2(CO)_2$ to the solution. The reaction was monitored by FT-IR, and the IR ν_{NO} stretching frequencies shifted from 1807 and 1760 cm^{-1} to 1684 and 1619 cm^{-1}. The reaction solution was filtered and washed with THF, and the solid was then dried under vacuum for several hours. Dark-green crystals, suitable for X-ray crystallography, were obtained by slow evaporation of the solution. Yield: 207 mg (86.4%). IR (Solid ATR): $\upsilon_{(NO)}$ 1684, 1619 cm^{-1}; ^{1}H NMR (DMSO-d_6, ppm): 8.66 (d, 2H), 8.32 (d, 2H), 8.21 (t, 2H), 7.54 (t, 2H); MS FAB: $[M]^+$ m/z = 272.05 (calc), 272.03 (expt).

Synthesis of Complex 2. Complex **2** was obtained using the 2,2′,2″-terpyridine by the same procedure as described above for **1**. Yield: 256 mg (81.5%). IR (Solid ATR): $\upsilon_{(NO)}$ 1688, 1621 cm^{-1}; ^{1}H NMR (DMSO-d_6, ppm): 9.21 (d, 1H), 8.69 (m, 2H), 8.58 (d, 1H), 8.40 (t, 1H), 8.07 (m, 3H), 7.47 (d, 1H), 7.07 (t, 1H); MS FAB: $[M]^+$ m/z = 349.14 (calc), 348.74 (expt).

Synthesis of Complex 3. Complex **3** was obtained using the 1,10-phenathroline by the same procedure as described above for **1**. Yield: 235 mg (88.2%). IR (Solid ATR): $\upsilon_{(NO)}$ 1686, 1614 cm^{-1}; ^{1}H NMR (DMSO-d_6, ppm): 8.86 (d, 2H), 8.40 (t, 2H), 8.19 (m, 2H), 7.74 (m, 4H); MS FAB: $[M]^+$ m/z = 296.07 (calc), 296.07 (expt).

Crystallography. Complexes **1** and **2** were glued to a thin glass fiber with epoxy resin and collected on a Bruker APEX II diffractometer equipped with a fine focus, 2.0 kW sealed tube X-ray source (Mo Kα radiation, λ = 0.7103 Å) operating at 50 kV and 30 mA at 273 K. The crystallographic collection and refinement parameters for complexes **1** and **2** are listed in Table 1. The empirical absorption correction was based on equivalent reflections, and other possible effects, such as absorption by the glass fiber, were simultaneously corrected. Each structure was solved by direct methods followed by successive difference Fourier methods. All non-hydrogen atoms were

(7) (a) McDonald, C. C.; Phillips, W. D.; Mower, H. F. *J. Am. Chem. Soc.* **1965**, *87*, 3319–3326. (b) Woolum, J. C.; Tiezzi, E.; Commoner, B. *Biochim. Biophys. Acta* **1968**, *160*, 311–320. (c) Butler, A. R.; Glidewell, C.; Li, M. *Adv. Inorg. Chem.* **1988**, *32*, 335–393, and references therein. (d) Dieck, H. T.; Bruder, H.; Kuhl, E.; Junghans, D.; Hellfeldt, K. *New J. Chem.* **1989**, *13*, 259–268. (e) Chatel, S.; Chauvin, A. S.; Tuchagues, J. P.; Leduc, P.; Bill, E.; Chottard, J. C.; Mansuy, D.; Artaud, I. *Inorg. Chim. Acta* **2002**, *336*, 19–28.

(8) (a) Basolo, F. *Polyhedron* **1990**, *9*, 1503–1535, and references therein. (b) Drapier, J. C.; Pellat, C.; Henry, Y. *J. Bio. Chem.* **1991**, *266*, 10162–10167. (c) Porasuphatana, S.; Weaver, J.; Budzichowski, T. A.; Tsai, P.; Rosen, G. M. *Anal. Biochem.* **2001**, *298*, 50–56. (d) Zhang, Y.; Oldfield, E. *J. Am. Chem. Soc.* **2004**, *126*, 4470–4471. (e) Tsou, C. -C.; Lu, T. -T.; Liaw, W. -F. *J. Am. Chem. Soc.* **2007**, *129*, 12626–12627. (f) Lu, T. T.; Tsou, C. C.; Huang, H. W.; Hsu, I. J.; Chen, J. M.; Kuo, T. S.; Wang, Y.; Liaw, W. -F. *Inorg. Chem.* **2008**, *47*, 6040–6050. (g) Chen, Y. J.; Ku, W. C.; Feng, L. T.; Tsai, M. L.; Hsieh, C. H.; Hsu, W. H.; Liaw, W. F.; Hung, C. H.; Chen, Y. J. *J. Am. Chem. Soc.* **2008**, *130*, 10929–10938.

(9) (a) Reginato, N.; McCrory, C. T. C.; Pervitsky, D.; Li, L. *J. Am. Chem. Soc.* **1999**, *121*, 10217–10218. (b) Wang, X.; Sundberg, E. B.; Li, L.; Kantardjieff, K. A.; Herron, S. R.; Lim, M.; Ford, P. C. *Chem. Commun.* **2005**, 477–479. (c) Huang, H. W.; Tsou, C. C.; Kuo, T. S.; Liaw, W. -F. *Inorg. Chem.* **2008**, *47*, 2196–2204.

(10) Hung, M. C.; Tsai, M. C.; Lee, G. H.; Liaw, W. F. *Inorg. Chem.* **2006**, *45*, 6041–6047.

(11) Braterman, P. S.; Song, J.-I.; Peacock, R. D. *Inorg. Chem.* **1992**, *31*, 555–559.

(12) Wah, H. L. K.; Postel, M.; Tomi, F.; Mordenti, L. *New J. Chem.* **1991**, *15*, 629–633.

(13) Wang, R.; Camacho-Fernandez, M. A.; Xu, W.; Zhang, J.; Li, L. *Dalton Trans* **2009**, 777–786.

(14) Heibner, W.; Beutner, H. *Z. Anorg. Allg. Chem.* **1963**, *320*, 101–111.

refined anisotropically. Computations were performed using SHELXTL, and final full-matrix refinements were performed against F^2. The SMART software was used for collecting frames of data, indexing reflections, and determination of lattice constants; SAINT-PLUS for integration of intensity of reflections and scaling; SADABS for absorption correction; and SHELXTL for space groups and structure determinations, refinements, graphics, and structure reporting.[15−17]

Electrochemistry. Cyclic voltammetry (CV) was carried out with a CH Instruments electrochemical analyzer 730A. A three-electrode system consisted of a platinum working electrode, a platinum wire counter electrode, and an Ag/Ag^+ reference electrode was used. The reference electrode was separated from the bulk of the solution by a fritted-glass bridge filled with the solvent/supporting electrolyte mixture. All CV data were recorded with the scan rate of 100 mV s^{-1} in THF with tetrabutylammonium hexafluorophosphate as the supporting electrolyte. All potential values are reported versus ferrocene/ferrocenium ion; and the $E_{1/2}°(Fc/Fc^+)$ under our experimental conditions are 0.20, 0.19, and 0.20 V for complexes **1**−**3**, respectively.

Results and Discussion

Synthesis of the Complexes. It has been demonstrated that the carbonyl groups of $Fe(NO)_2(CO)_2$ can be easily replaced by phosphorus-containing or sulfur-containing ligands to produce the dinitrosyl complexes as reported in previous studies.[13,18] In rare cases, it can be replaced by nitrogen-contained ligands.[9,10] To prepare and isolate a new class of DINC containing N,N′-chelating ligands and to investigate their properties, a series of DNICs $[Fe(NO)_2(bipy)]$, $[Fe(NO)_2(terpy)]$, and $[Fe(NO)_2(phen)]$ were prepared, as shown in Scheme 1, by the reaction of $Fe(NO)_2(CO)_2$ with the appropriate ligand in THF at ambient temperature. All reactions were performed under N_2 atmosphere in a glovebox and were monitored by FT-IR spectroscopy. Upon the addition of $Fe(NO)_2(CO)_2$ to the solution containing ligands, a great amount of bubbles were produced, and the characteristic IR absorptions of nitroysl groups (ν_{NO}) were shifted to lower frequencies as the carbonyls were being replaced by the ligands. The observations are consistent with the results obtained from MS, NMR, and single crystal X-ray diffraction. Complex **1** was obtained as a green solid with 86.4% yield, while complexes **2** and **3** were isolated as brick red solids with 81.5% and 88.2% yield, respectively. X-ray quality single crystals for **1** and **2** were obtained by slow evaporation of the solvent, THF, or methanol. Complexes **1**−**3** are stable in the solid state under nitrogen, and all three complexes are relatively soluble in most polar organic solvents including dichloromethane, methanol, and THF, but are insoluble in diethyl ether and hexane.

Spectroscopic Characterization. The infrared spectra of **1**−**3** were recorded in THF solution and in solid (ATR)

Scheme 1

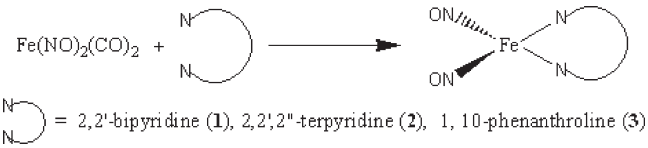

(Supporting Information, Figure S1). Upon reacting with the ligands, the typical carbonyl stretching frequencies (ν_{CO}, 2087 and 2037 cm^{-1}) from the start material, $Fe(NO)_2(CO)_2$, disappeared, indicating that both carbonyl groups are replaced by the bidentate ligands 2,2′-bipyridine, 2,2′,2″-terpyridine, or 1,10-phenathroline as observed in the crystal studies. In the meantime, the characteristic IR absorptions of nitroysl groups ($\nu_{NO,}$ 1807, 1760 cm^{-1}) shifted ∼120−146 wavenumbers to 1684 cm^{-1} and 1619 cm^{-1} for **1**, 1688 cm^{-1} and 1621 cm^{-1} for **2**, and 1686 cm^{-1} and 1614 cm^{-1} for **3**, respectively. These values are located in the range of NO^+,[19] suggesting that these nitrogen-containing ligands act as strong σ donors rather than π-acceptors. The peaks close to 1619 cm^{-1}, 1621 cm^{-1}, and 1614 cm^{-1} in complexes **1**−**3** are assigned to the coordinated bidentate ligands by comparing them with the IR spectra of the free ligands. The characteristic nitrosyl stretching frequencies are similar to the reported values 1673 cm^{-1}, 1616 cm^{-1} for the mononuclear metal complex $Fe(NO)_2$(sparteine)[10] and 1679 cm^{-1}, 1622 cm^{-1} for $Fe(NO)_2(1\text{-MeIm})_2$;[9a] but clearly lower than the values 1774 cm^{-1}, 1712 cm^{-1} for the anionic complex[9c] $[Fe(NO)_2(Im\text{-}H)_2]^-$, and 1796 cm^{-1}, 1726 cm^{-1} for the tetranuclear iron complex[9b] $[Fe(NO)_2(Im\text{-}H)]_4$. The results show that the NO stretching frequencies are related to the oxidation levels of DNICs and the observed ν_{NO}s' in complexes **1**−**3** make them $\{Fe(NO)_2\}^{10}$ according to the Enemark−Feltham notation.[20]

The ^1H NMR and ^{13}C NMR spectra of the complexes **1**−**3** were recoded in DMSO (Supporting Information, Figure S2−S4). The ^1H NMR of complex **1** shows four sets of resonances between 7.54 ppm and 8.66 ppm, and the ^{13}C NMR shows five distinct peaks in the aromatic carbon region, which are assigned to the coordinated bipy ligand. Complex **3** exhibits four sets of resonances between 7.74 and 8.86 ppm with two of them very close to each other, and the ^{13}C NMR shows six distinct carbons which correspond to the protons and carbons in the coordinated phen ligands, respectively. The NMR results indicate that both complexes **1** and **3** possess high symmetry. On the contrary, complex **2** displays seven sets of resonances between 7.07 and 9.21 ppm, which are attributed to the magnetic inequivalence of the three pyridyl rings in the terpy ligand, meaning this compound bears low symmetry. These observations are consistent with the results found in the crystal structures of complexes **1** and **2**, which show that the two NOs are symmetrically located on two sides of the Fe(bipy) plane in complex **1**, while in complex **2**, the two NOs are

(15) *SMART and SAINT for Windows NT Software Reference Mannuals*, Version 5.0; Bruker Analytical X-Ray Systems: Madison, WI, 1997.

(16) Sheldrick, G. M. *SADABS − A Software for Empirical Absorption Correction*; University of Göttingen: Göttingen, Germary, 1997.

(17) *SHELXTL Reference Manual*, Version 5.1; Bruker Analytical X-Ray Systems: Madison, WI, 1997.

(18) (a) Hörsken, A.; Zheng, G.; Stradiotto, M.; McCrory, C. T. C.; Li, L. *J. Organomet. Chem.* **1998**, *558*, 1–9. (b) Li, L. *Comments Inorg. Chem.* **2002**, *23*, 335–353. (c) Li, L.; Reginato, N.; Urschey, M.; Stradiotto, M.; Liarakos, J. D. *Can. J. Chem.* **2003**, *81*, 468–475.

(19) Wang, P. G.; Cai, T. B.; Taniguchi, N. *Nitric Oxide Donors*; Wiley-VCH: New York, 2005.

(20) (a) Enemark, J. H.; Feltham, R. D. *Coord. Chem. Rev.* **1974**, *13*, 339–406. (b) Richter-Addo, G. B.; Legzdins, P. *Metal Nitrosyls*; Oxford University Press: Oxford, U.K., 1992, p 81. (c) Liaw, W. F.; Chiang, C. Y.; Lee, G. H.; Peng, S. M.; Lai, C. H.; Darensbourg, M. Y. *Inorg. Chem.* **2000**, *39*, 480–484.

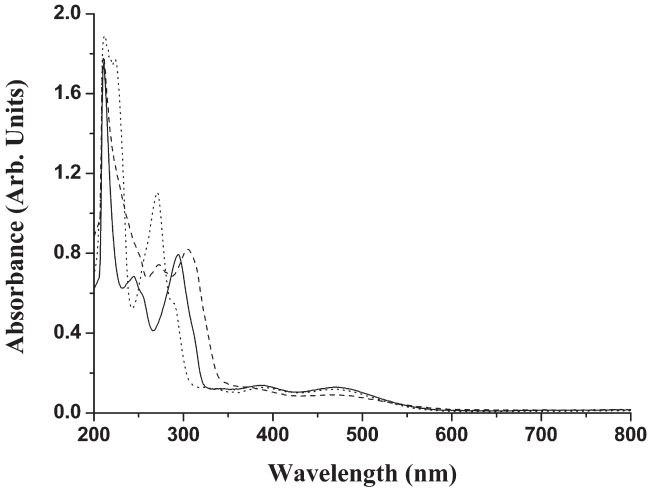

Figure 1. Electronic absorption spectra of complexes **1** (solid), **2** (dash), and **3** (dot) in THF.

distributed in two sides of the plane consisting of Fe and two coordinated pyridyl rings but almost parallel to the uncoordinated pyridyl ring.

The electronic absorption spectra of complexes **1**−**3** are shown in Figure 1. Complex **1** shows one strong absorption at 211 nm, two medium absorptions at 245 and 294 nm, and two weak absorptions at 390 and 471 nm. It is similar to the spectrum of **2**, which displays one strong absorption at 211 nm, two medium absorptions at 272 and 304 nm, and two weak absorption bands at 374 and 470 nm. Complex **3** reveals two strong absorptions at 212 and 224 nm, one medium absorption at 271 nm, one shoulder at 290 nm, and two weak absorption bands at 389 and 470 nm. These absorptions mainly arise from the transitions between orbitals delocalized over the bidentate [N,N] ligands (N,N-L), ligand to metal charge transfer (LMCT) (π^*_{NO}-d_{Fe}, $\pi^*_{N,N\text{-}L}$-d_{Fe}), and metal to ligand charge transfer (MLCT) (d_{Fe}-π^*_{NO}, d_{Fe}-$\pi^*_{N,N\text{-}L}$).[11,21] The relative low-energy absorption bands at 374−471 nm can be assigned mainly to the MLCT (d_{Fe}-π^*_{NO}, d_{Fe}-$\pi^*_{N,N\text{-}L}$), while the absorptions at higher energy are attributed to combined contributions from LMCT (π^*_{NO}-d_{Fe}, $\pi^*_{N,N\text{-}L}$-d_{Fe}), π_{NO} ($\pi_{N,N\text{-}L}$)→ d_{Fe}, π_{NO}→ π^*_{NO}, and ligand-localized transitions of the coordinated [N,N] ligands, $\pi_{N,N\text{-}L}$→$\pi^*_{N,N\text{-}L}$.

Electrochemical Properties. The redox behavior of complexes **1**−**3** was studied by CV in THF. The experiments were performed with a three-electrode system (Platinum working electrode, Platinum counter electrode, and $Ag/AgNO_3$ reference electrode) and tetrabutylammonium hexafluorophosphate as the supporting electrolyte. The half-wave potentials for these complexes are presented in Table 2. As shown in Figure 2, complex **1** exhibits two quasi-reversible one-electron reductions at −0.48 V and −2.07 V [versus $E_{1/2}{}^{\circ}{}_{(Cp2Fe/Cp2Fe+)}$], while complexes **2** and **3** show two quasi-reversible one-electron reductions at −1.09 V, −2.07 V and −0.50 V, −2.05 V, and one irreversible reduction at −1.85 V and −1.80 V, respectively. The first reductions of all complexes are

(21) (a) Bourassa, J.; Lee, B.; Bernard, S.; Schoonover, J.; Ford, P. C. *Inorg. Chem.* **1999**, *38*, 2947–2952. (b) Jaworska, M.; Stasicka, Z. *J. Mol. Struct.* **2006**, *785*, 68–75.

Table 2. Redox Potentials of Complexes **1**−**3**[a] Determined by CV

complex	$E^{\circ}{}_{1/2,\ expt}$(V) (vs Fc^+/Fc)		
1	−0.48		−2.07
2	−1.09	−1.85[b]	−2.07
3	−0.50	−1.80[b]	−2.05

[a] Condition: 1 mmol dm^{-3} THF solution at ambient temperature, 0.1 mol dm^{-3} $[Bu_4N]PF_6$, scan rate of 100 mV s^{-1}, platinum working electrode. [b] Irreversible redox of a solvated species.

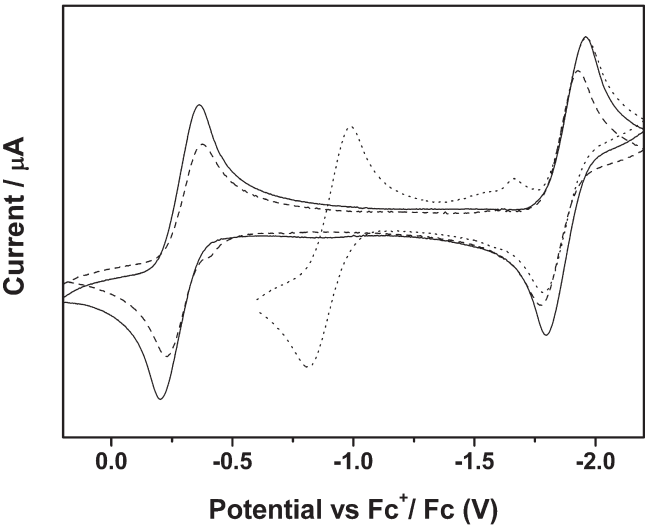

Figure 2. Cyclic voltammograms of a 1 mM solution of complex **1** (solid), **2** (dot), and **3** (dash) in 0.1 M $[NBu_4][PF_6]$/THF.

assigned to the $[LFe(NO)_2]/[LFe(NO)_2]^-$ couple, while the reductions close to −2.07 V are believed to be the usual ligand-based reductions.[11] The half-wave potential of the first reduction peak for complex **2** is clearly more negative than the corresponding values for complexes **1** and **3**, showing that complex **2** is more difficult to reduce. It is consistent with the greater electron donor effect of the uncoordinated pyridyl ring in complex **2**. The results indicate that the electronic property of the ligands has important influence on the electrochemical properties of the relevant complexes.

It should be pointed out that the peak intensity of the second reduction is very small in comparison with the first and third ones for complexes **2** and **3**. Since the purity of samples has been confirmed by NMR spectra, the unusual peaks are thought to be from a solvated species. To demonstrate this hypothesis, different concentrations of complex **2** solutions were used to perform the electrochemical test, and the results are shown in Figure 3. As expected, the CV showed that the intensities of the first and third reduction peaks clearly decreased when the concentrations descended from 1.0 mM to 0.25 mM, but the second reduction peak at −1.85 V did not change much. The relative intensities for the second reduction increased with the addition of solvent, indicating that it is indeed a solvated species. This is consistent with the experimental observations that the solubility of those complexes is clearly bigger in the coordinating solvents such as methanol, THF, and acetonitrile. A similar phenomenon has also been found in our previous investigations for the tetranuclear iron complex $[Fe(NO)_2(Im\text{-}H)]_4$.[9b] The studies show that this kind of DNIC, which

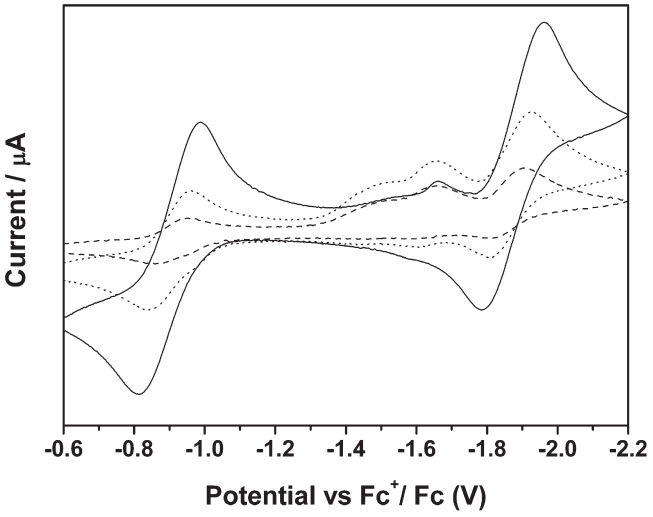

Figure 3. Cyclic voltammogram of complex **2** with the concentrations of 0.25 (dash), 0.50 (dot), and 1.0 mM in 0.1 M $[NBu_4][PF_6]$/THF.

Table 3. Selected Bond Lengths (Å) and Bond Angles (deg) for Complexes **1** and **2**

1		**2**	
Fe1−N1	1.652(4)	Fe1−N4	1.643(3)
Fe1−N2	1.647(4)	Fe1−N11	1.652(3)
Fe1−N3	2.050(4)	Fe1−N1	2.053(2)
Fe1−N4	2.042(4)	Fe1−N5	2.042(2)
N1−O1	1.183(5)	N4−O16	1.189(3)
N2−O2	1.188(5)	N11−O24	1.193(3)
Fe1−N1−O1	169.0(4)	Fe1−N4−O16	172.0(3)
Fe1−N2−O2	166.7(4)	Fe1−N11−O24	172.1(3)
N1−Fe1−N2	114.4(2)	N4−Fe1−N11	118.89(13)
N3−Fe1−N4	78.45(15)	N1−Fe1−N5	78.55(9)
O1−Fe1−O2	104.25	O16−Fe1−O24	112.4
N1−Fe1−N3	111.20(17)	N1−Fe1−N11	110.96(11)
N2−Fe1−N4	114.91(18)	N4−Fe1−N5	109.04(11)

bears nitrogen-contained ligands, has the tendency to solvate in the coordinating solvents.

Structural Studies. The molecular structures of complexes **1** and **2** have been determined by X-ray diffraction analysis, and the selected bond lengths and bond angles are listed in Table 3. They are all neutral based on the X-ray resolved molecular formula. As shown in Figure 4, complex **1** crystallizes in the triclinic $P\bar{1}$ space group, and the asymmetric unit consists of one $Fe(NO)_2$(bipy) molecule with NO groups in the two sides of Fe(bipy) plane. Each iron center is connected to four nitrogen atoms, which include two from the nitrosyls and two nitrogen atoms from the bipy ligands, with a pseudotetrahedral geometry. The average $Fe-N_{(NO)}$ bond distance of 1.650 Å is similar to those reported in mononuclear complexes $Fe(NO)_2$(sparteine) (average value: 1.646 Å),[10] $[(MeIm)_2Fe(NO)_2]$ (MeIm = 1-methylimidazole) (average value: 1.649 Å),[9a] and $[(DAD)Fe(NO)_2]$ (DAD = diazadiene) (average value: 1.641 Å)[7d]but clearly shorter than those found in the tetranuclear $[Fe(NO)_2(Im\text{-}H)]_4$ (Im = imidazole) (average value: 1.694 Å)[9b] and the dinuclear complexes, $[(N_2C_5H_7)Fe(NO)_2]_2$ ($N_2C_5H_7$ = 3,5-dimethylpyrazolyl) (average value: 1.696 Å),[22] in which the iron is considered to carry one positive charge to balance the negative charge on the

(22) Chong, K. S.; Rettig, S. J.; Storr, A.; Trotter, J. *Can. J. Chem.* **1979**, *57*, 3119–3125.

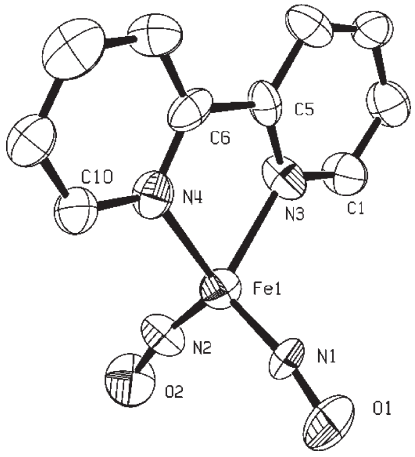

Figure 4. Molecular structure of complex **1** with thermal ellipsoids drawn at the 50% probability.

nitrogen-contained ligands due to deprotonation. This positive Fe center would have less electrons available for back-donation to the nitrosyl ligands, resulting in weaker Fe−N bonds. The Fe−N−O groups are symmetrically bent with the average $O_{(NO)}-Fe1-O_{(NO)}$ and $N_{(NO)}-Fe1-N_{(NO)}$ angles of 104.2° and 114.4°, respectively. These are considered "attracto" conformations because the N−Fe−N bond angles are less than 120° and the two oxygen atoms are bent toward each other.[6c] It is consistent with the suggestion that the "attracto" conformations are generally favored in first-row transition-metal dinitrosyls with π-accepting ligands.[22] The average Fe−N−O bond angle of 167.9° is thought to be close to linear formation, indicating that the nitrosyl moieties exhibit sp hybridized NO^+ character in complex **1**;[19]while the $N_{(N,N\text{-}L)}-Fe1-N_{(N,N\text{-}L)}$ bond angle of 78.4° shows that the Fe(N4) possesses severe distorted tetrahedral environment.

The crystal packing diagram of complex **1** reveals a layering effect in which different layers interact by the $\pi-\pi$ stacking and H-bonding effects (Figure 5). The $Fe(NO)_2$(bipy) molecules of different layers are staggered with iron nitrosyls in the opposite sides. Interestingly, the two aspectrant bipyridine rings almost completely overlap, which is expected because the space hindrance is compensated by the H-bonding interactions of nitrogen and oxygen atoms of nitrosyls with the hydrogen atoms from the adjacent bipyridine ligands. As shown in Figure 6, the distance is 3.5880 Å between planes I and II, and 3.6264 Å between planes II and III, indicating that there are quite strong $\pi-\pi$ stacking interactions between the two aspectrant bipyridine ligands, but the interactions are stronger inside the separate units consisting of two $Fe(NO)_2$(bipy) molecules than between the separate units. The supramolecular structure is formed based to these associated factors in the crystal packing structure.

Complex **2** crystallizes in the monoclinic $P21/n$ space group, and the asymmetric unit contains one $Fe(NO)_2$(terpy) molecule (Figure 7). Similar to the complex **1**, each iron center is also connected to four nitrogen atoms, which include two from the nitrosyls and two nitrogen atoms from the terpy ligands. The uncoordinated pyridyl is perpendicular with the plane consisting of an iron atom

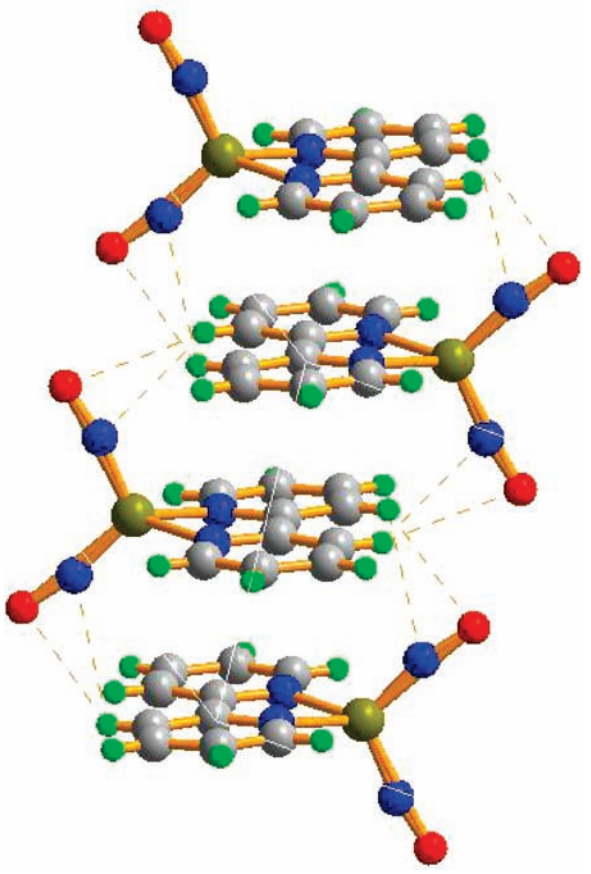

Figure 5. Packing structure of complex **1** showing the $\pi-\pi$ stacking and H-bonding interactions.

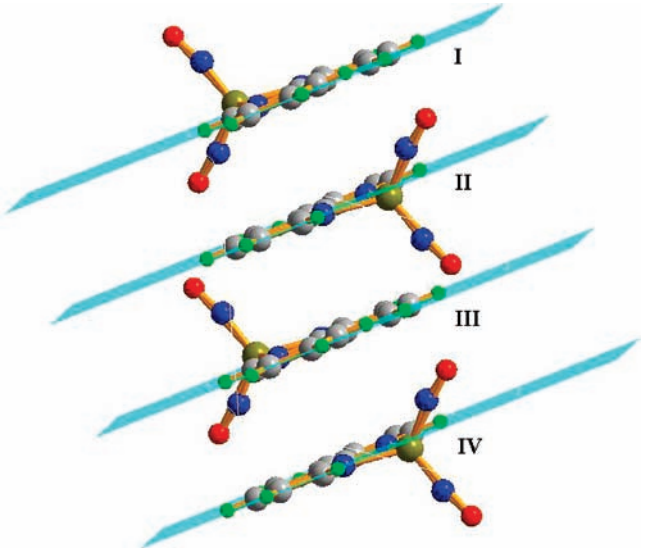

Figure 6. Packing structure of complex **1** showing the plane of different layers with $\pi-\pi$ stacking interactions.

and two coordinated pyridyl rings, but almost parallel to the $Fe(NO)_2$ plane. The average $Fe-N_{(NO)}$ and $Fe-N_{(N,N\text{-}L)}$ bond lengths are 1.648 Å and 2.048 Å, respectively, which are comparable to the relevant 1.650 Å and 2.046 Å in complex **1**. Complex **2** also exhibits an "attracto" conformation with the angles of 104.0° and 114.9° for O−Fe−O and $N_{(N,N\text{-}L)}-Fe-N_{(N,N\text{-}L)}$, respectively. In both complexes **1** and **2**, $Fe-N_{(NO)}$ bond distances are all clearly shorter than $Fe-N_{(N,N\text{-}L)}$ distances, indicating the NO groups are much better π-acceptors than either 2,2′-bipyridine or 2,2′,2″-terpyridine.

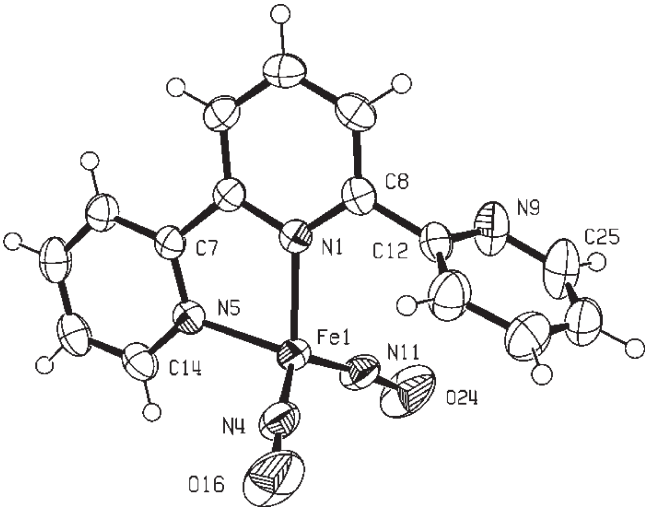

Figure 7. Molecular structure of complex **2** with thermal ellipsoids drawn at the 50% probability.

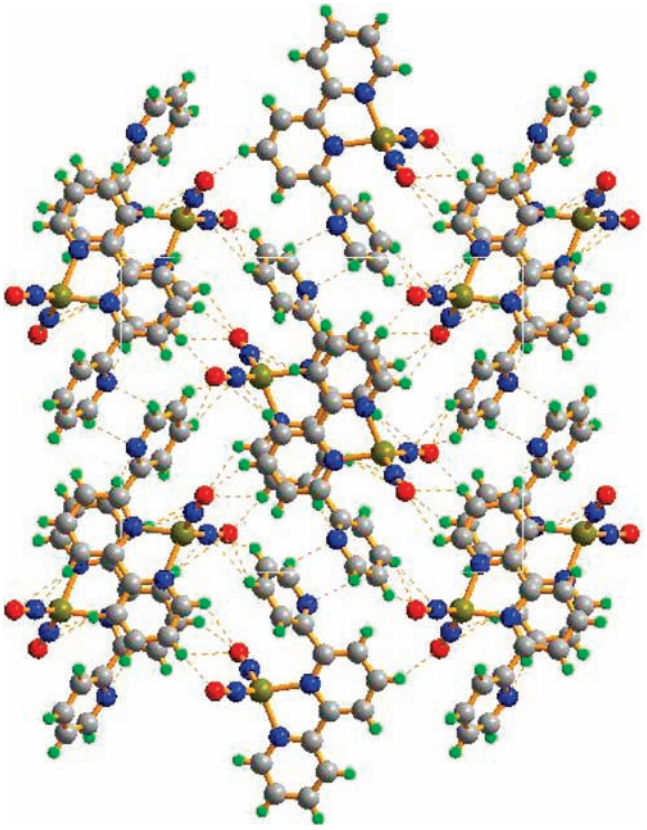

Figure 8. Packing structure of complex **2** showing the $\pi-\pi$ stacking and H-bonding interactions viewed along the *a*-axis.

As shown in Figure 8, the packing diagram of complex **2** also exhibits $\pi-\pi$ stacking and H-bonding interactions. Analogous to complex **1**, The $Fe(NO)_2$(terpy) molecules of different layers are also staggered to make the uncoordinated pyridyl away from each other and the iron nitrosyls in the opposite sides. The two coordinated pyridyl rings of

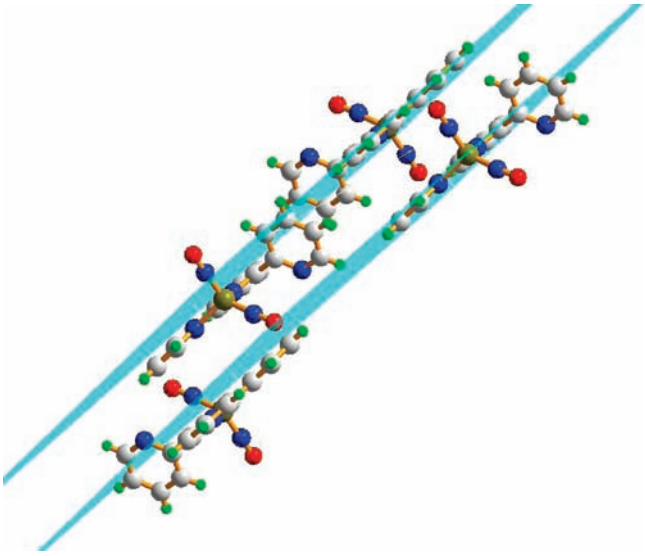

Figure 9. Part of packing structure of complex **1** showing the plane of different layers with $\pi-\pi$ stacking interactions.

terpyridine ligands almost completely overlap with the opposite one with a distance of 3.4254 Å (Figure 9), but almost no interactions are observed between the adjacent uncoordinated pyridyls (the interval: 4.3569 Å).

Conclusions

Three DNICs, $LFe(NO)_2$ (L = 2,2′-bipyridine (bipy) (**1**), 2,2′,2″-terpyridine (terpy) (**2**), and 1,10- phenathroline (phen) (**3**)), were synthesized by the reaction $Fe(NO)_2(CO)_2$ with the corresponding ligands in THF and were studied by IR, UV−vis, MS, NMR, and electrochemistry. Complexes **1** and **2** were also characterized using single crystal X-ray diffraction analysis. IR spectra of complexes **1**−**3** displayed two strong characteristic NO stretching frequencies (ν_{NO}) in solid with the characteristic of NO^+. The electronic absorption spectra all show five main bands in the range of 211−471 nm, which are assigned to the transitions between orbitals delocalized over the bidentate [N,N] ligands (N, N-L), LMCT (π^*_{NO}-d_{Fe}, $\pi^*_{N,N-L}$ -d_{Fe}) and MLCT (d_{Fe}-π^*_{NO}, d_{Fe}-$\pi^*_{N,N-L}$). CV showed two quasi-reversible one-electron reductions for the complexes **1**−**3** and an irreversible reduction from a solvated species for complexes **2**−**3**. The results are coincident with the experimental observation that the solubility of those complexes is clearly larger in the coordinating solvents such as methanol, THF, and acetonitrile. Single-crystal X-ray structural analysis revealed that complex **1** crystallizes in triclinic $P\bar{1}$ space group and the asymmetric unit consists of one $Fe(NO)_2$(bipy) molecule with NO groups in the two sides of Fe(bipy) plane, while complex **2** crystallizes in the monoclinic $P21/n$ space group and the asymmetric unit contains one $Fe(NO)_2$(terpy) molecule, in which NO groups locate on two sides of the plane consisting of Fe and two coordinated pyridyl rings but almost parallel to the uncoordinated pyridyl ring. In addition, intermolecular H-bonding and $\pi-\pi$ stacking interactions were observed in both complexes.

Acknowledgment. We wish to thank the National Institute of Health (NIH) MBRS SCORE Program (Grant #2 S06 GM 063119) for financial support.

Supporting Information Available: IR, NMR, and MS spectra of complexes **1**−**3**, and the X-ray crystallographic files in CIF format for the structure determinations of complexes **1** and **2**. This material is available free of charge via the Internet at http://pubs.acs.org.